GAMB-D-73-0069

J. Phys. F: Metal Phys., Vol. 3, January 1973. Printed in Great Britain. © 1973.

Changes in the Fermi surfaces of zinc and cadmium subjected to uniaxial compression

D Gamble and B R Watts

School of Mathematics and Physics, University of East Anglia, Norwich NOR 88C, UK

MS received 18 August 1972

Abstract. The changes produced by uniaxial compression in the Fermi surfaces of zinc and cadmium have been measured using a new device for applying the compressive stress. The de Haas–van Alphen effect was used to determine the changes in the smaller extremal orbits, four in zinc and three in cadmium. Where comparison is possible, satisfactory agreement is obtained with other work. One orbit in zinc, whose position on the Fermi surface was formerly uncertain, is more reliably identified from the results.

1. Introduction

During the past few years there have been reported a number of experiments on the changes produced in the Fermi surfaces of metals which have been elastically stressed. In the majority of experiments the changes in Fermi surface have been determined from measurements on quantum oscillations (particularly the de Haas–van Alphen effect) in crystals which have been subjected to pressure or uniaxial stress.

Metals which have been studied under pressure are: potassium, rubidium, caesium (Glinski and Templeton 1969); copper, silver, gold (Templeton 1966, Schirber and O'Sullivan 1970b): beryllium (Schirber and O'Sullivan 1969a); zinc (Balain *et al* 1960, O'Sullivan and Schirber 1966); cadmium (Schirber and O'Sullivan 1968); aluminium (Meltz 1966); lead (Anderson *et al* 1967a); indium (O'Sullivan *et al* 1967 and 1968); tin (Perz *et al* 1969); thallium (Anderson *et al* 1970); graphite (Anderson *et al* 1967b); antimony (Schirber and O'Sullivan 1969b, Tay and Priestley 1970); bismuth (Itskevich and Fisher 1968, Schirber and O'Sullivan 1970a); tungsten (Schirber 1971); zirconium (Schirber 1970).

Metals which have been studied under uniaxial stress are: copper, silver, gold (Shoenberg and Watts 1967); gold (Gamble and Watts 1972); tin (Perz and Hum 1971); bismuth (Brandt and Ryabenko 1960, Bate and Einspruch 1965).

The effect of uniaxial stress has been deduced in a number of metals by combining measurements of the amplitude of de Haas–van Alphen oscillations with measurements of the amplitude of the equivalent oscillations in the magnetostriction. Metals studied in this way have been: copper, silver, gold (Slavin 1972); beryllium (Chandrasekhar *et al* 1967); zinc (Griessen and Kundig 1972, Reitz and Sparlin 1972); aluminium (Griessen and Sorbello 1972); bismuth (Aron and Chandrasekhar 1969).

Measurements of the velocity of sound have also yielded results for the pressure dependence of the Fermi surface of beryllium (Testardi and Condon 1970).

We shall describe in some detail a new method of applying elastic uniaxial compression to single metal crystals. The method requires careful specimen preparation which will also be described.

The de Haas–van Alphen effect has been used, in a way similar to that of Shoenberg and Watts (1967), to measure the changes produced in the Fermi surfaces of zinc and cadmium when the uniaxial compression is applied parallel to the $\langle 0001 \rangle$ crystalline axis. Our results will be compared with other work on these metals, referred to above.

2. Experimental technique

2.1. General considerations

The de Haas–van Alphen effect is the oscillatory behaviour of the magnetic moment of metals which occurs when the applied magnetic field $\boldsymbol{B}$ is varied. Generally the oscillations which are periodic in $1/B$ contain several distinct frequencies F_i, each of which is proportional to an extreme cross sectional area A_i of the Fermi surface sectioned perpendicular to $\boldsymbol{B}$;

$$F_i = \alpha A_i$$

where α is a constant. Therefore the changes produced in F_i when stress σ is applied to a crystal give a measure of the changes produced in the Fermi surface, according to the following relations

$$\frac{\partial \ln A_i}{\partial \sigma} = \frac{\partial \ln F_i}{\partial \sigma} = \frac{\partial \ln \phi_i}{\partial \sigma} \tag{1}$$

where $\phi_i = 2\pi F_i/B$ is the phase of the oscillations.

In our experiments we were concerned to ensure that only elastic strain was produced. Therefore we did not exceed strains of order 10^{-4}, corresponding to stresses of order 10^7 N m^{-2}. Now, the larger sections of metal Fermi surfaces, comparable with a free electron sphere, have values of F sufficiently high that in fields of order 5 T, as used in practice, the phase would be $2\pi \times 10^4$. Therefore, if we assume that these larger sections scale approximately as would a free electron sphere, the strain applied would be capable of producing phase changes of order 2π. The phase change is usually of the same order for small sections of the Fermi surface because the fractional area change produced by a given stress is much greater.

In our experiments we measured the changes $\delta\phi_i$ produced by uniaxial compressional stress. Although there is some difficulty in measuring $\delta\phi_i$ with high precision, the most important technical problem is to ensure that when the stress is applied the measured $\delta\phi_i$ is due to the change produced in the size and shape of the Fermi surface and not due to rotational or translational motion of the specimen in the magnetic field. Careful specimen preparation and experimental design are needed and these will be described later. However, since we restricted our measurements to symmetry direction orbits (specifically $\boldsymbol{B}$ along $\langle 0001 \rangle$) the change of F with angle, and hence any spurious change of ϕ_i due to crystal rotation, was minimized. Furthermore we concerned ourselves only with the smaller orbits where frequencies have an inherently lower sensitivity to rotation or translation of the crystal. A further reason for ignoring the larger orbits was that their de Haas–van Alphen oscillations were often of very small amplitude; perhaps because of the inevitable cold working of the sample when it was initially stressed.

Although we have therefore ignored the larger parts of the Fermi surface, this is perhaps not too serious an omission because theoretical descriptions of the Fermi surface and its strain derivatives are most sensitively tested by the smaller pieces.

2.2. Mechanical

The apparatus used for applying uniaxial compression is shown in figure 1 and figure 2 (plate). An important feature of the design is that the pull rod does not pass through a vacuum seal to get inside the cryostat because the whole lever arm is enclosed in the vacuum tight box. It would seem that omitting the vacuum seal in this way is worthwhile in order to ensure that the stress applied to the specimen is accurately known (Gamble and Watts 1972). The lever arm had twenty equally spaced notches on to which a $\frac{1}{2}$ kg weight could be hung and we were thus able to increase the compressional force from approximately zero to 10 kg weight in $\frac{1}{2}$ kg weight steps. The weight was moved in a way very similar to that in which the rider is moved along the arm of a conventional sensitive weighing balance. The jaws, between which the specimen is compressed, are such that the upper one is machined accurately perpendicular to the suspension axis and the lower jaw is machined perpendicular to the axis of the bottom moving part of the suspension. There is a small residual play left in the pins which connect this lower part to the pull rod, in order to allow the jaws to be self aligning with the flat ends of the specimen when the compressional force is applied.

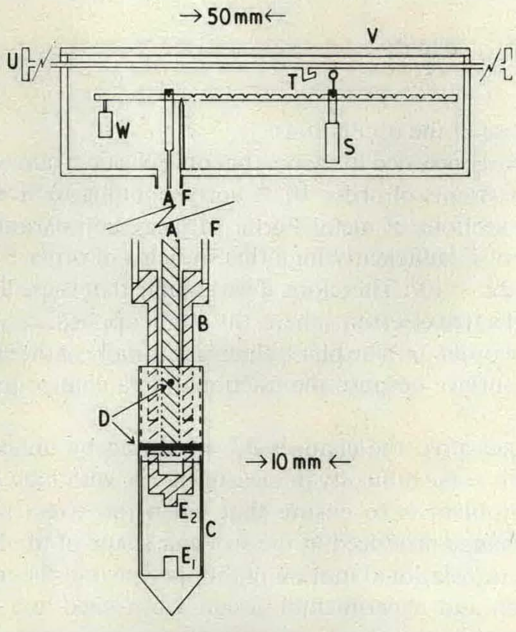

Figure 1. The stainless steel pull rod A is coupled directly to C by the pins D. The pins D pass through slots in B, enabling tension in A to produce compression between the moving jaw E_1 and the jaw E_2 which is held stationary (by the stainless steel tube F) with respect to the lever arm pivot. The weight S may be lifted by engaging T and rotating slightly the rod U. S is moved to different notches on the lever arm by sliding U along. The process is viewed through the perspex window V. W is a counter balance weight. The lever arm enclosure is vacuum tight. Various vacuum seals have not been shown. Note the scales are different for the two parts of the figure.

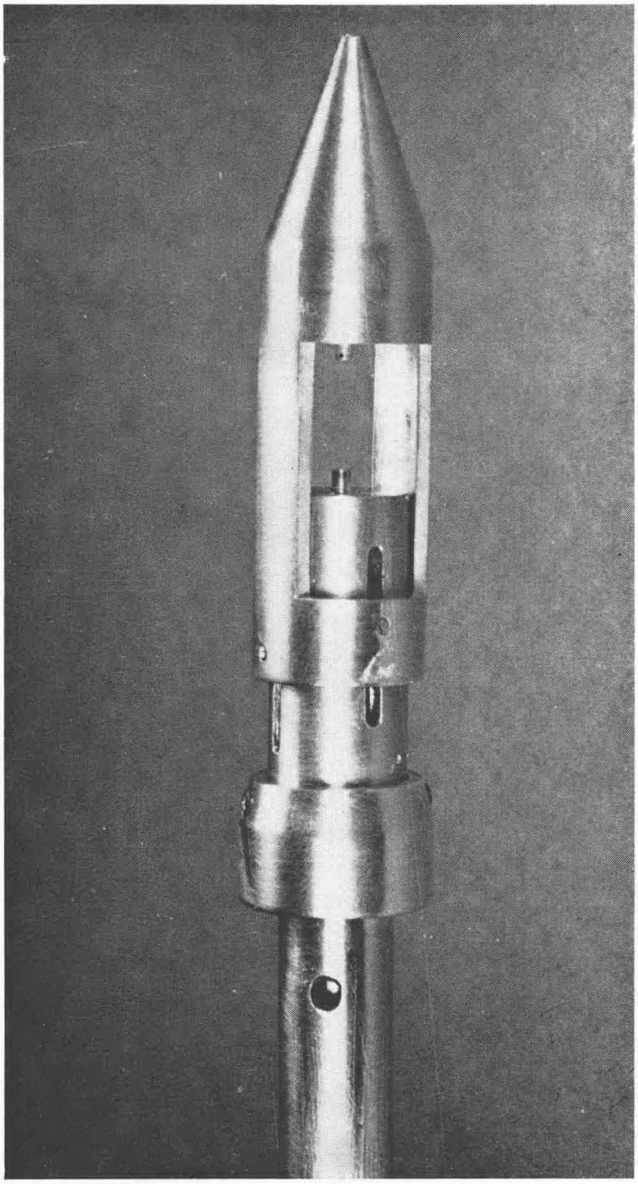

Figure 2. Photograph of a compression apparatus. This is not the apparatus actually used but differs only slightly in some absolute and relative dimensions.

Although our apparatus for producing compression is more complicated at the bottom end than the tension apparatus of Shoenberg and Watts (1967) or Perz and Hum (1971), we felt that this was more than compensated for by being able to dispense with the difficulties of having to solder, glue or clamp our specimens in position.

2.3. Specimens

The specimens used were right cylinders approximately 2 mm in diameter and between 4 mm and 6 mm in length. For our compression experiments it is obvious that we require the ends of the specimens to be flat, parallel to each other and to $\{0001\}$ and that the long axis be parallel to $\langle 0001 \rangle$. The following procedure was followed to obtain these requirements.

The zinc or cadmium started as a large roughly cylindrical single crystal ingot about 25 mm in diameter. Using x rays for orientation determination, a spark erosion machine was used to cut from the ingot a slice whose plane was within a few degrees of $\{0001\}$, and whose thickness was of order 5 mm.

The next step was to spark plane one face of the slice to be exactly parallel to $\{0001\}$. This was done by mounting the rough slice on an adjustable jig in which it was first x rayed and then planed on the spark erosion machine. The jig was designed to be mountable on both the x ray machine and the spark machine and was itself accurately machined so that the axis of rotation of the spark wheel would be exactly parallel to the axis of the x ray beam when it was transferred from one device to the other. Therefore, it was only necessary to adjust the movable part of the jig until the $\{0001\}$ back reflection Laué spot was in the centre of the x ray picture and then transfer the jig to the spark machine where the face was planed.

In order to plane the second face parallel to the first, the slice was turned over and fixed to a plane surface which had itself been planed parallel to the planing wheel. The second face of the slice was then planed, with the slice in this position.

Cylindrical specimens were cut from the slice with a suitably sized tube cutter in the place of the planing wheel. On each cut the tube cutter was stopped just before it reached the bottom of the disc. When a sufficient number were nearly cut out in this way, the slice was turned over again, glued down and planed off until the specimens were separated from the slice. We adopted this rather complicated method for finally separating the specimens from the slice because if the tube cutter were allowed to cut right through then in the final stages the specimens were liable to tip over and be ruined.

2.4. de Haas–van Alphen detection system

The de Haas–van Alphen oscillations were detected using a conventional low frequency AC field modulation system based on the radio frequency technique of Shoenberg and Stiles (1964). The modulation frequency was usually about 230 Hz, although this was sometimes increased to about 1 kHz to improve signal to noise ratio.

The magnetic field was produced by a superconducting solenoidal magnet with a maximum field of 6 T. The homogeneity quoted by the manufacturers, but not checked, was better than 3 parts in 10^4 over the central centimetre sphere.

The de Haas–van Alphen oscillations were plotted out against magnetic field on an X–Y recorder as shown in figure 3. Because it is difficult to measure the magnetic field directly, the voltage we used to produce the X displacement was obtained from across a resistor placed in series with the magnet current supply. Although this was an easy and convenient thing to do, it suffered from the disadvantage that it would have created experimental errors if there had been any hysteresis in the relation between magnetic field in the solenoid and its energizing current. However, we took precautions in connection with this which are described in §2.5.

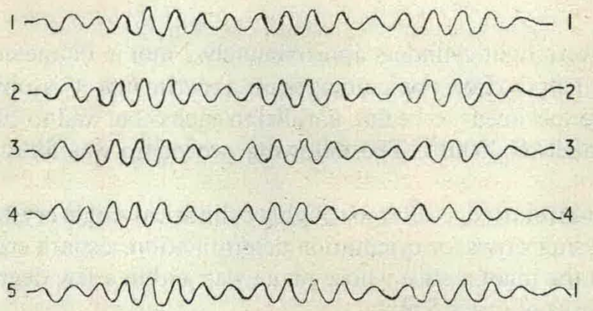

Figure 3. A series of recordings of the α oscillations in zinc with various applied compressional forces. The numbers on the left give the order in which the recordings were made, and the numbers on the right the compressional force in kg weight. All recordings were made with B increasing (left to right) from about 2·7 T to 3·0 T. The amplitude modulation is due to beating with the weaker β oscillations.

We inserted a field back off voltage into the X displacement input of the recorder so that we could expand relatively small variations of magnetic field in order to examine the oscillations in detail.

2.5. Experimental procedure

Initially, setting up adjustments were made to the detection system to maximize the de Haas–van Alphen signal to noise ratio which was further improved by pumping the liquid helium to about 1·2 K.

The position of the specimen holder was then progressively changed until the specimen was in the centre of the magnetic field. During this process the position was monitored by measuring the amplitude of the signal as the specimen holder was moved along the magnet axis in steps of approximately 1 mm. Accuracy in this adjustment is potentially important since the application of tension to the pull rod (producing compression of the specimen) will slightly shorten the whole specimen holder and thereby raise the specimen in the field. Calculation suggests that the spurious change in phase thus produced would be negligible provided the specimen was within a few mm of the field centre to start with. This restriction would have been more severe if we had studied higher de Haas–van Alphen frequencies.

No further adjustments were made and the change of phase with stress was measured as follows. The procedure was to sweep B over a suitable range and plot out a number of oscillations, say about 20, with a very small compression ($T_0 \sim \frac{1}{2}$ kg weight) applied. The field was then swept back to its starting value though two recordings were not usually made with both increasing and decreasing B. The compression T was then increased in steps of say 1 kg weight and at each value of T a recording of the oscillations was made as described above. Finally T was reduced to T_0 and a recording of the oscillations made again. A series of such recordings is shown in figure 3.

The sensitivity of the phase to stress was calculated directly by measuring the changes in position δx of the turning points when the compression was changed. It is straightforward to show that, if the change in compressional force is ΔT, then

$$\frac{\partial \ln \phi}{\partial \sigma} = \frac{a\,\delta x/B}{b\Delta T} \tag{2}$$

where a is a calibration factor which converts changes of position δx into equivalent changes of B and b is a factor (depending on the cross sectional area of the specimen) which converts changes of T into changes of σ. Equations (1) and (2) were used to find the stress sensitivity of the Fermi surface from measurements of δx. Generally δx and B were taken to be the mean values over a field sweep since this introduced no significant error. However, it was necessary to be more careful for the needles in zinc since B varied by a large fraction from turning point to turning point. In this case $\delta x/B$ was evaluated at each turning point and the average of this quotient taken afterwards.

Errors in our experimental results arose primarily from determining δx, though some error from the measurement of B as well as from a and b are included in the results.

The errors in B, a and b were routine; however it is worth discussing certain precautions taken in connection with the above procedure to ensure that spurious phase changes ($\propto \delta x$) were not being produced by the recording system. The most likely source of trouble would have been that the field–current relation of the magnet was irreproducible. We were able to check on this by doing a number of preliminary field sweeps at fixed T to check on the reproducibility of the phases of the oscillations as plotted. It was never possible to obtain reproducible results when comparing up and down sweeps. However, it was always possible to get more or less identical up (or down) sweeps provided that the range of B swept was kept approximately constant. In fact a reason for always returning to a final T_0 sweep at the end of a series was to check that the phases were unchanged from the initial T_0 sweep.

Another potential source of recording error was the possibility of long term drift in the back off on the X displacement of the X–Y recorder. Again, the plotting of the final T_0 plots would have shown up any steady drift of this kind. Shorter term fluctuations capable of producing a shift of the curves to left or right were also monitored by ensuring that on each sweep a given field current (determined by a high sensitivity digital voltmeter) always corresponded to a fixed X displacement. Occasionally slight long term drift was observed but this was measured and allowed for in measurements of δx.

Random errors, produced by the difficulty of estimating the maxima and minima of the curves, were calculated by measuring and comparing all the turning points (except those near the ends) and it was found that these random errors were always appreciably larger than any likely systematic errors in the detection system.

Nevertheless, consistency experiments on a single specimen could not rule out the possibility that the specimen was systematically rotating, for example, when compression was applied to it. We therefore used two or more specimens and compared results from different specimens. Since the differences between specimens were not significant in comparison with the random errors, there is no reason for believing that errors due to rotation or translation of the specimens were important.

Another potential error arising from the mechanical system was that on the first application of stress there was sometimes some amplitude reduction accompanied by an irreversible change of phase, due, presumably, to plastic effects. This source of error was automatically checked by the procedure of always returning at the end of a sequence to T_0 and checking the phase. However, a preliminary application and removal of stress was always made as this seemed to ensure elastic behaviour thereafter.

It is worth comparing the phase observation technique of Shoenberg and Watts (1967) in which they obtained very high field stability by using their magnet in the persistent mode. For the most part they were studying high de Haas–van Alphen frequencies. Since these have a very small field interval between oscillations, a high field stability was required but only a small field sweep was necessary to display the oscillations. Therefore their persistent mode technique is ideal, because the limitation that it has too small field sweeps does not matter. However, for lower frequencies such as we have studied the field stability criterion is proportionately lower, whereas the need for a larger sweep range is proportionately greater. Therefore, in our experiments we adopted the different procedure described above.

We were able to observe several de Haas–van Alphen frequencies with $\boldsymbol{B}$ along $\langle 0001 \rangle$ but in order to measure phase changes of the weaker ones it was necessary to filter out the ones of higher amplitude. We did this generally by using a variable low frequency electronic filter in the output of the detection system. This filter was adjusted to accept the frequency of interest. In two cases (the α and β oscillations in both zinc and cadmium to be described) where two close frequencies produced beats (figure 3) we determined the phase change of the dominant oscillation directly and inferred the other by measuring the shift in the beat pattern.

3. Results

3.1. General

Our experimental apparatus restricted our studies to extremal orbits lying in $\{0001\}$ planes through the Fermi surfaces. The compressional stress along $\langle 0001 \rangle$ retains the hexagonal symmetry of the Brillouin zone but increases its volume and its height (along $\langle 0001 \rangle$) and reduces its width.

The Fermi surfaces and the observed orbits in zinc and cadmium are discussed by Fletcher *et al* (1969) with references to other work.

We shall tabulate our results in three alternative forms. The most straightforward form $\partial \ln \partial\sigma$, is obtained directly from the experiment.

The second form is the ratio of the measured fractional area change to the theoretical fractional change for a free electron sphere of cross sectional area A_s

$$\frac{\partial \ln A_s}{\partial\sigma} = \frac{2}{3}\frac{\partial \ln V}{\partial\sigma}$$

where V is the volume of the Brillouin zone. We used the appropriate low temperature elastic constants to calculate the dimensionless quantity $\partial \ln A/\partial \ln A_s$ which would take values close to $+1$ for orbits which are like those on the free electron sphere. It is worth noticing how our results, which are from small orbits, differ from $+1$ in both magnitude and sometimes sign.

The third form is used to make an objective comparison of our results with other work on the sensitivity of the orbits to hydrostatic pressure and thermal expansion. We observe that uniaxial compression produces a change in the axial ratio c/a. However, because of the large anisotropy of the elastic constants, hydrostatic pressure and thermal expansion also produce changes in the c/a ratio. Therefore, we can express all three kinds of experiments in a common way, in terms of $\partial \ln A/\partial(c/a)$.

3.2. *Zinc*

The zinc orbits studied were the following:

(i) the first zone hole pocket at H (α orbit). The existence of this pocket is not in doubt but there does not seem to have been reported an unambiguous observation of this orbit before;

(ii) the junction at H of the diagonal arms of the second zone hole surface (β orbit);

(iii) the waist of the needles, the third zone electron surface at K (N orbit);

(iv) the unidentified orbit labelled C by Fletcher *et al* (C orbit). For reasons discussed in §3.4 we believe that this is a magnetic breakdown orbit round the diagonal arms in the second zone.

Our results are listed in table 1, which also includes other experimental results.

The α and β oscillations were observed as beats with α having the greater amplitude. The β result in table 1 was calculated from measurements of phase change of the beat

Table 1. Results in zinc

Orbit	$10^2 \times \frac{\partial \ln A}{\partial \sigma}$ (kbar^{-1}) Present	Magnetostriction	$\frac{\partial \ln A}{\partial \ln A_s}$ Expt	Theory	$\frac{\partial \ln A}{\partial (c/a)}$ Present	Pressure	Temp
α	$-3{\cdot}34 \pm 0{\cdot}09$		-41 ± 1	-16			
β	$-3{\cdot}5 \pm 0{\cdot}3$		-44 ± 3	-16			
N	85 ± 10	78 ± 5 (GK) 60 ± 2 (RS)	1060 ± 120	410	-150 ± 18	-166 ± 8	-190 ± 30
C	$-2{\cdot}5 \pm 0{\cdot}2$		-31 ± 2	$-9{\cdot}3$ (A) $+19$ (B)			

The magnetostriction results are by Griessen and Kundig (1972), and by Reitz and Sparlin (1972). The pressure result is the average of measurements made by Balain *et al* (1960) and O'Sullivan and Schirber (1966); these results are consistent with each other. The temperature result is by Berlincourt and Steele (1954). The two theoretical results for the C orbit are respectively for the second zone hole monster arms (A) and for the third zone electron butterflies (B).

pattern, combined with the phase change of the α oscillations. Combination of errors from these two independent measurements leads to the larger error on the β result. The low temperature elastic constants used to calculate entries in the table were measured by Alers and Neighbours (1958).

3.3. *Cadmium*

The cadmium orbits studied are listed below using the orbit labels of Tsui and Stark (1966):

(i) the first zone pocket at H (α orbit);

(ii) the junctions at H of the diagonal arms of the second zone hole surface (β orbit);

(iii) the large orbit in the ΓKM plane round the second zone hole surface ($\gamma^{1/3}$ orbit). It is interesting to note that we observe the $\gamma^{1/3}$ orbit to be very much stronger than $\gamma^{2/3}$ or γ, as also do Fletcher *et al* in their ultrasonic attenuation experiments. This is in marked disagreement with Tsui and Stark who found $\gamma^{2/3}$ to be strongest. However, there seems

Table 2. Results in cadmium

Orbit	$-10^2 \times \frac{\partial \ln A}{\partial \sigma}$ (kbar^{-1})	$\frac{\partial \ln A}{\partial \ln A_s}$ Expt	$\frac{\partial \ln A}{\partial \ln A_s}$ Theory	$\frac{\partial \ln A}{\partial (c/a)}$ Present	$\frac{\partial \ln A}{\partial (c/a)}$ Pressure
α	-2.58 ± 0.07	-28.2 ± 0.8	-17	4.2 ± 0.1	4.0 ± 0.4
β	-2.62 ± 0.12	-28.6 ± 0.13	-17	4.2 ± 0.2	3.6 ± 0.4
$\gamma^{1/3}$	$+0.67 \pm 0.03$	$+7.3 \pm 0.3$	-2.0	-1.08 ± 0.05	-0.4 ± 0.2

The pressure results are by Schirber and O'Sullivan (1968).

to be no reason to doubt their assignment of the orbit. Our results are listed in table 2 where they are compared with other experimental work. The β orbit was measured in the same way as the β orbit in zinc and for the same reason the error is relatively large. The low temperature elastic constants used in calculating entries in the table were measured by Garland and Silverman (1960, 1962).

3.4. Discussion

We see that where comparison is possible there is generally good agreement between our results and those of others. However it should be noted that only the magnetostriction results on the needles in zinc are directly comparable with our results, whereas the pressure and temperature results have had to be compared in terms of the derived quantity $\partial \ln A/\partial(c/a)$. We would not necessarily expect a given change of c/a to produce identical effects when the change in c/a is produced in different ways as it is here. However, we believe that the observed agreement is due to the large anisotropy of the elastic constants in zinc and cadmium which means that quite similar volume changes correspond to a given c/a ratio change whether this is produced by pressure, uniaxial stress or temperature.

As regards the magnetostriction results on the needles in zinc, there is much better agreement with the results of Griessen and Kundig than with those of Reitz and Sparlin. However, there is some reason for believing the results of Griessen and Kundig to be more reliable. Reitz and Sparlin themselves note that they can make a direct comparison of their results with the pressure results of O'Sullivan and Schirber but find unsatisfactory agreement. But, if they had used the value of Griessen and Kundig given in our table, they would have obtained excellent agreement.

A natural way to interpret our results would be to adopt a pseudopotential approach and to calculate the changes of Fermi surface in terms of the changes produced in the shape and size of the Brillouin zone and the changes produced in the pseudopotential coefficients. However, this is quite a complicated programme of work and requires a considerable computational effort. Therefore we have listed the results of a much simpler calculation, in which we have made the nearly free electron approximation. In this approximation we assume that the topology of the Fermi surface is governed by the Brillouin zone but that the band gaps are zero. The calculation is thus reduced to simple geometry.

Though we would not expect any striking agreement between our simple theory and experiment, we note that there is general agreement both in sign and general trend with the exception of the $\gamma^{1/3}$ orbit of cadmium. However, since the topology of the Fermi surface in the region of this orbit differs from the nearly free electron prediction, the discrepancy with regard to this orbit is not at all surprising.

As regards the C orbit in zinc, the sign and magnitude of the experimental result are helpful in deciding between alternative assignments suggested by Fletcher *et al.* They suggest that the C orbit may either be round an electron surface in the third zone called the butterfly, or a magnetic breakdown orbit involving the arms of the second zone hole surface and the first zone hole surface. Their figure 6 shows that the latter orbit consists for most of its length of a second zone hole orbit and therefore, if this were the correct interpretation of the C orbit, we would expect it to have a similar sensitivity to strain as the β orbit which is nearby on the same surface. On the other hand the butterflies are electron overlaps into the third zone around L and inspection of their position relative to that of the second zone arms makes it seem probable that the sensitivities of two alternatives to strain would have opposite sign.

In the table 1 we have given the theoretical calues for both alternative assignments. We observe that these have opposite signs, and looking at the kind of agreement in the table obtained for the β orbit, there seems to be no real doubt that given the alternatives the orbit is to be associated with the second zone hole surface. Indeed it is gratifying that the butterflies need not be invoked since pseudopotential calculations fitted to known de Haas–van Alphen data (Stark and Falicov 1967) rule out the existence of the butterflies.

4. Conclusion

We have used a new technique to measure the changes produced in the Fermi surfaces of zinc and cadmium by uniaxial compression along the ⟨0001⟩ axis. We have not attempted any detailed theoretical interpretation, although we have shown that the trend of the results is generally consistent with nearly free electron theory.

It has also been possible to use the sign of one of our results to distinguish plausibly between two alternative orbits round the Fermi surface as the origin of a particular set of de Haas–van Alphen oscillations in zinc.

Our results have been compared with other results for the changes of Fermi surface produced by hydrostatic pressure, temperature and uniaxial stress. Good agreement is obtained.

Acknowledgments

We would like to thank Dr Z S Basinski of the National Research Council of Canada for providing the single crystal ingots of zinc and cadmium from which our specimens were prepared.

References

Alers G A and Neighbours J R 1958 *J. Phys. Chem. Solids* **7** 58–64

Anderson J R , O'Sullivan W J and Schirber J E 1967a *Phys. Rev.* **153** 721–5

Anderson J R, O'Sullivan W J, Schirber J E and Soule D E 1967b *Phys. Rev.* **164** 1038–42

Anderson J R, Schirber J E and Stone D R 1970 *Propriétés Physiques des Solides sous Pression* (Paris: Centre National de la Recherche Scientifique) pp 131–7

Aron P R and Chandrasekhar B S 1969 *Phys. Lett.* **30A** 86–7

Balain K S, Grenier C G and Reynolds J M 1960 *Phys. Rev.* **119** 935–8

Bate R T and Einspruch N G 1965 *Phys. Lett.* **16** 11–12
Berlincourt T G and Steele M C 1954 *Phys. Rev.* **95** 1421–8
Brandt N B and Ryabenko G A 1960 *Sov. Phys.–JETP* **10** 278–9
Chandrasekhar B S, Fawcett E, Sparlin D M and White G K 1967 *Proc. Tenth Int. Conf. Low Temp. Phys., Moscow* 328–32
Fletcher R, MacKinnon L and Wallace W D 1969 *Phil. Mag.* **20** 245–58
Gamble D and Watts B R 1972 *Phys. Lett.* **40A** 22
Garland C W and Silverman J 1960 *Phys. Rev.* **119** 1218–22
—— 1962 *Phys. Rev.* **127** 2287
Glinski R and Templeton I M 1969 *J. low temp. Phys.* **1** 223–9
Griessen R and Kundig A 1972 *Solid St. Commun.* **11** 295–8
Griessen R and Sorbello R S 1972 *Phys. Rev.* B **6** 2198–208
Itskevich E S and Fisher L M 1968 *Sov. Phys.–JETP* **26** 66–70
Meltz P J 1966 *Phys. Rev.* **152** 540–7
O'Sullivan W J and Schirber J E 1966 *Phys. Rev.* **151** 484–94
O'Sullivan W J, Schirber J E and Anderson J R 1967 *Solid St. Commun.* **5** 525–8
—— 1968 *Phys. Lett.* **27A** 144–5
Perz J M and Hum R H 1971 *Can. J. Phys.* **49** 1–8
Perz J M, Hum R H and Coleridge P T 1969 *Phys. Lett.* **30A** 235–6
Reitz L M and Sparlin D M 1972 *Phys. Rev.* B **5** 3803–7
Schirber J E 1970 *Phys. Lett.* **33A** 172–3
—— 1971 *Phys. Lett.* **35A** 194–5
Schirber J E and O'Sullivan W J 1968 *Proc. Eleventh Int. Conf. Low Temp. Phys., St. Andrews* pp 1141–4
—— 1969a *Phys. Rev.* **184** 628–34
—— 1969b *Solid St. Comm.* **7** 709–11
—— 1970a *Phys. Rev.* B **2** 2936–40
—— 1970b *Propriétés Physiques des Solides sous Pression* (Paris: Centre National de la Recherche Scientifique) pp 113–21
Shoenberg D and Stiles P J 1964 *Proc. R. Soc.* **281A** 62–91
Shoenberg D and Watts B R 1967 *Phil. Mag.* **15** 1275–88
Slavin A J 1972 to be published
Stark R W and Falicov L M 1967 *Phys. Rev. Lett.* **19** 795–8
Tay C Y and Priestley M G 1970 *Propriétés des Solides sous Pression* (Paris: Centre National de la Recherche Scientifique) pp 139–42
Templeton I M 1966 *Proc. R. Soc.* **292A** 413–23
Testardi L R and Condon J H 1970 *Phys. Rev.* B **1** 3928–42
Tsui D C and Stark R W 1966 *Phys. Rev. Lett.* **16** 19–22